Molecular modelling approaches for designing inhibitors of L-amino acid oxidase from *Crotalus adamanteus* venom

Jyotirmoy Mitra, Kanika Sharma and Debasish Bhattacharyya*

Division of Structural Biology and Bioinformatics, CSIR-Indian Institute of Chemical Biology, 4, Raja S.C. Mallick Road, Jadavpur, Kolkata 700 032, India

L-amino acid oxidase (LAAO) from snake venom induces diverse toxicity into the victims, which is attributed to H_2O_2 generated during the catalytic conversion of L-amino acids. In this study, homology model of LAAO from *Crotalus adamanteus* has been compared with the crystal structure of LAAO from *Calloselasma rhodostoma*. The root mean square deviations obtained from superposition of the FAD-binding, substrate-binding and helical domains of LAAO from *Crotalus adamanteus* with those of LAAO from *Calloselasma rhodostoma* crystal structure confirmed a high degree of structural similarity between them. Based on the interactions of the substrate, L-phenylalanine and the reversible inhibitor, *o*-aminobenzoic acid with the catalytic residues of LAAO from *Calloselasma rhodostoma*, five probable inhibitors were designed. AutoDock Vina program was employed to perform automated molecular docking of these probable inhibitors. Two of them emerged as reversible inhibitors with IC_{50} values of 1.6 and 3.3 μM respectively.

Keywords: Docking, molecular modelling, snake venom toxins, suicide substrate, L-amino acid oxidase.

SNAKE bite is a major neglected health issue within poor communities of tropical countries. According to an estimate, yearly 2.5 million people are bitten by snakes worldwide. Among them, 0.125 million victims die[1]. The cost, unavailability, instability and lack of efficacy of anti-venom therapy has resulted in the development of alternate methods for snakebite management. Development of better therapeutics can be initiated by understanding the mode of action and catalytic mechanism of different toxins present in venom and generating specific inhibitors to neutralize the venom toxins. Snake venom L-amino acid oxidases (SV-LAAO) (EC 1.4.3.2) are flavoenzymes that catalyse stereospecific oxidative deamination of L-amino acids to α-keto acid via α-imino acid intermediate along with generation of ammonia and hydrogen peroxide (H_2O_2) (Figure 1 *a*)[2]. The enzyme has attracted considerable attention due to its multifunctional nature. High abundance of the enzyme in snake venom causes toxicity as it induces impairment of platelet aggregation together with necrotic and apoptotic type of cell death[3]. This effect is primarily attributed to the production of high concentration of H_2O_2 localized on the cell surface[4,5]. LAAO from *Crotalus adamanteus* and *Crotalus atrox* can associate specifically with mammalian endothelial cells, possibly through the glycosylation site of the enzyme[4,6]. Recently, LAAO from the Malayan pit viper has been shown to induce both necrosis and apoptosis in Jurkat cells, where the role of H_2O_2 was well established by scavenging it with catalase[7]. It was predicted that the glycan moiety of LAAO is used in binding the enzyme to the cell surface, thus enhancing the localization of H_2O_2 (refs 4, 6).

The enzymes from snake venom exhibit a marked preference for hydrophobic amino acids like phenylalanine, tryptophan, tyrosine and leucine as substrate[3,8]. This substrate preference originates from the binding of hydrophobic side chains of amino acids with the enzyme. Recent crystallographic studies of LAAO from *Calloselasma rhodostoma* complexed with L-Phe and *o*-aminobenzoic acid (OAB) revealed that the catalytic site of each subunit of the dimeric enzyme is composed of three parts: a FAD-binding domain, a substrate-binding domain and a helical domain[9,10]. High degree of structural similarity of these three domains of LAAO from *Calloselasma rhodostoma*, *Bothrops jararacussu* and *Bothrops moojeni* was observed through comparative sequence homology and molecular modelling[11]. Also, LAAO from *Calloselasma rhodostoma* shares 84% sequence identity with that of *Crotalus adamanteus*. Overall, snake venom LAAOs are highly conserved with respect to their structure, function and substrate specificity.

Flavin-dependent enzymes are efficiently inhibited by substrate analogues which fulfil the criteria for suicide substrate, also known as mechanism-based inhibitor[12–15]. These inhibitors are compounds having chemical and structural features resembling those of the normal substrate of an enzyme. In addition, they contain a functional group which is converted to a highly reactive species within the active site of the enzyme during catalysis. This reactive moiety can inactivate the enzymes either by modifying the cofactor or a reactive amino acid residue

*For correspondence. (e-mail: debasish@iicb.res.in)

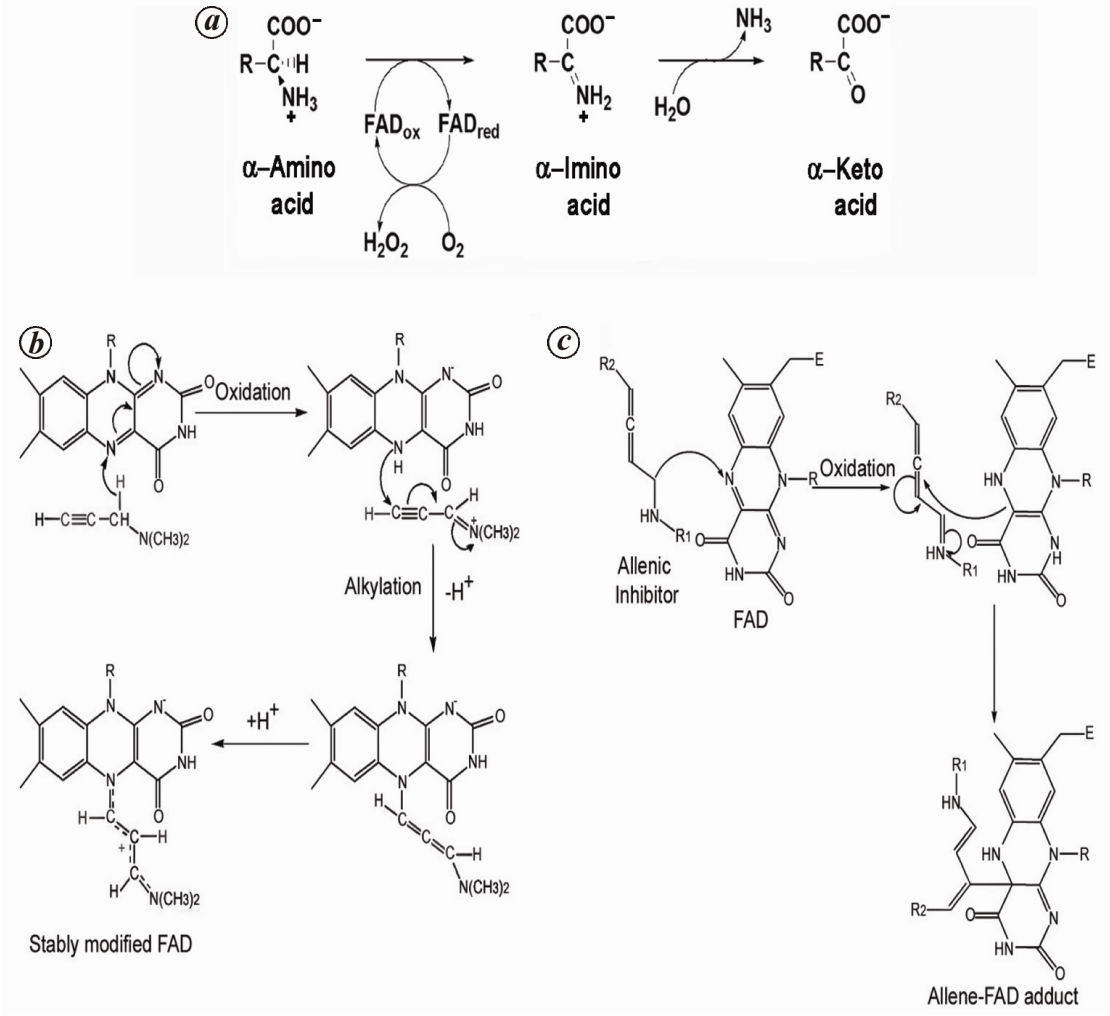

Figure 1. Irreversible modification of FAD bound to LAAO. ***a***, Nucleophilic attacks from N5 of isoalloxazine ring of FAD leads to stable FAD-inhibitor adduct. ***b***, Instead of N5, in this case a neighbouring C-atom plays the role of the nucleophile. In both cases, a non-electrophilic substrate analogue is converted into a strong electrophile during the catalysis process. An oxidative imine intermediate formation is essential for activation of such inhibitors. ***c***, Catalysis of LAAO. The first half reaction involves conversion of FAD to $FADH_2$ with concomitant oxidation of the amino acid to an imino acid. The unstable imino acid is then hydrolysed by the enzyme-bound water to form the final product, keto acid. An oxidative half reaction completes the catalytic cycle by reoxidizing FADH2 with oxygen, producing hydrogen peroxide.

during catalytic turnover[16,17]. A number of potent mechanism-based inhibitors are used as marketed drugs, e.g. clorgyline, selegiline and rasagiline. Clorgyline irreversibly inhibits mono amine oxidase (MAO) A and is used as an antidepressant drug, whereas the other two inactivate MAO-B isoforms. They have great therapeutic potency against Parkinson's disease[18–20]. The mechanism of modification of the flavin residue by such acetylenic and allenic inhibitors is shown in Figure 1 *b* and *c*. Success of such flavoenzyme inhibitors and inhibition of SV-LAAO by L-propargylglycine has generated an interest in developing a second set of suicide substrates[21]. Based on phenylalanine and OAB structures, five acetylenic derivatives were designed and synthesized. Docking of these molecules at the catalytic site of LAAO model provides useful structural insight into the binding interaction of the inhibitors with the catalytic residues.

Materials and methods

Materials

Fine chemicals were procured as follows: phenyl pyruvic acid, propargylamine, propargyl bromide, 2-carboxybenzaldehyde, formaldehyde and 2-amino benzoic acid methyl ester from Sigma, USA; sodium cyanoborohydride from Fischer, USA, and dry dimethylformamide (DMF) from E. Merck, India. All other reagents and solvents were of analytical grade and purchased locally. *Crotalus adamanteus* (Eastern Diamondback rattle snake) venom was

purchased from Sigma, USA and LAAO was purified as described previously[21].

Molecular modelling

Amino acid sequence of LAAOs from *Crotalus adamanteus* was retrieved from UniProtKB/Swiss Prot database (www.uniprot.org) (protein database O93364). These sequences were aligned with other snake venom LAAOs such as *Agkistrodon halys* (PDB ID: 1REO)[22], *Vipera ammodytes ammodytes* (PDB ID: 3KVE)[23] and *Calloselasma rhodostoma* (PDB ID: 2IID)[10] using 'ClustalW2.1' (http://www.ebi.ac.uk/Tools/msa/clustalw2). The crystal structure of *Calloselasma rhodostoma* (2IID) LAAO was downloaded from the Protein Data Bank (PDB). A set of two homology models were built using 'Swiss model' and 'CPH model' on-line server, where 2IID served as reference template structure[24,25]. The structure that was derived from homology modelling was validated by ProSA – a tool that is widely used to check 3D models of protein structures for potential errors[26,27]. The homology model of *Crotalus adamanteus* LAAO that was generated using CPH model server was refined by incorporating FAD at the catalytic site using the coordinates defined in 2IID pdb structure. Three main domains – FAD-binding, substrate-binding and helical domains of the homology model were superimposed on the respective domains of the crystal structure and root mean square (RMS) deviations were calculated.

Inhibitor designing and docking study

Crystallographic structures of SV-LAAO complexed with the reversible inhibitor *o*-aminobenzoate and the substrate L-Phe provided important insight into the mode of substrate and inhibitor binding to the enzyme and the possible mechanism of catalysis[9,10]. The substrate L-Phe is bound to the reface of the cofactor FAD and the side chain of L-Phe is accommodated in a sub-pocket which is constituted of the side chains of Ile374, His223 and Arg322 residues (Figure 2), i.e. benzene ring has good affinity at the sub-pocket. The carboxylate group and the amino group of the substrate and inhibitor interact with the hydrophilic residues of the catalytic funnel[9,10]. For catalysis, α-C atom of the substrate should be positioned over the isoalloxazine ring at a distance of 3.1 Å from N5 atom of FAD for proper hydride transfer to take place. This is also assisted by the carboxylate group and the amino group of the substrate. Structures of MAO inhibitors were designed using similar molecular interactions and currently they are used as drugs[20] (Figure 3 *a*). These data encourage designing of inhibitors that contain aromatic benzene ring, carboxylic group and amino group, so that the molecule is guided through the catalytic funnel up to the catalytic site. A major advantage of using L-Phe and OAB scaffold for the designing of LAAO inhibitors is that they are well recognized by the catalytic site of LAAO and hence can be exploited further for designing more potent inhibitors. However, OAB scaffold is associated with structural limitation such as lack of tetrahedral α-C atom that hinders its binding to the active site in a substrate-like fashion. The structures of probable inhibitors are shown in Figure 3 *b*.

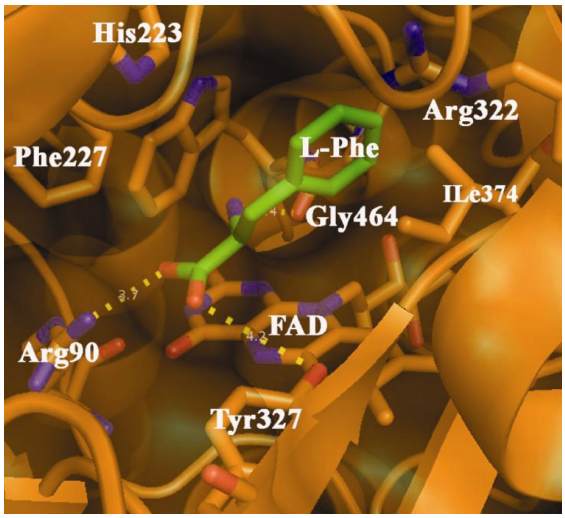

Figure 2. Catalytic site of *Calloselasma rhodostoma* LAAO showing the interaction of bound L-phenylalanine ligand (PDB ID: 2IID).

Structures of inhibitors were drawn using Chem Draw ultra 6.0 software and the corresponding pdb structures of the inhibitors were manually generated in Chem 3D ultra. All docking experiments were performed using AutoDock Vina software. AutoDock toolkit was used to prepare the models for docking[28,29]. In the homology model, hydrogen atoms were added and Gasteiger charge model was used for protein and FAD. To account for the side-chain flexibility during docking, flexible torsions in the ligands were assigned, Gasteiger charge was added and the α-C atom was allowed to rotate freely. Then the receptor (homology model of LAAO) and the ligand (inhibitors) were saved in PDBQT format for the AutoDock Vina program. The default parameters of Vina were used for docking simulation. However, exhaustiveness was set to 30 and a docking grid of 30, 30 and 30 points (1 point = 1 Å) in the x, y and z directions was built which encompassed the entire LAAO active site and centred on FAD cofactor. In other words, a cube of 30 Å arm length was created around FAD. Finally the lowest energy binding conformation was analysed and illustrated using Pymol[30].

Synthesis of proposed inhibitors and in vitro enzyme assay

Syntheses of inhibitors were carried out at 25°C under nitrogen or argon atmosphere, unless mentioned otherwise.

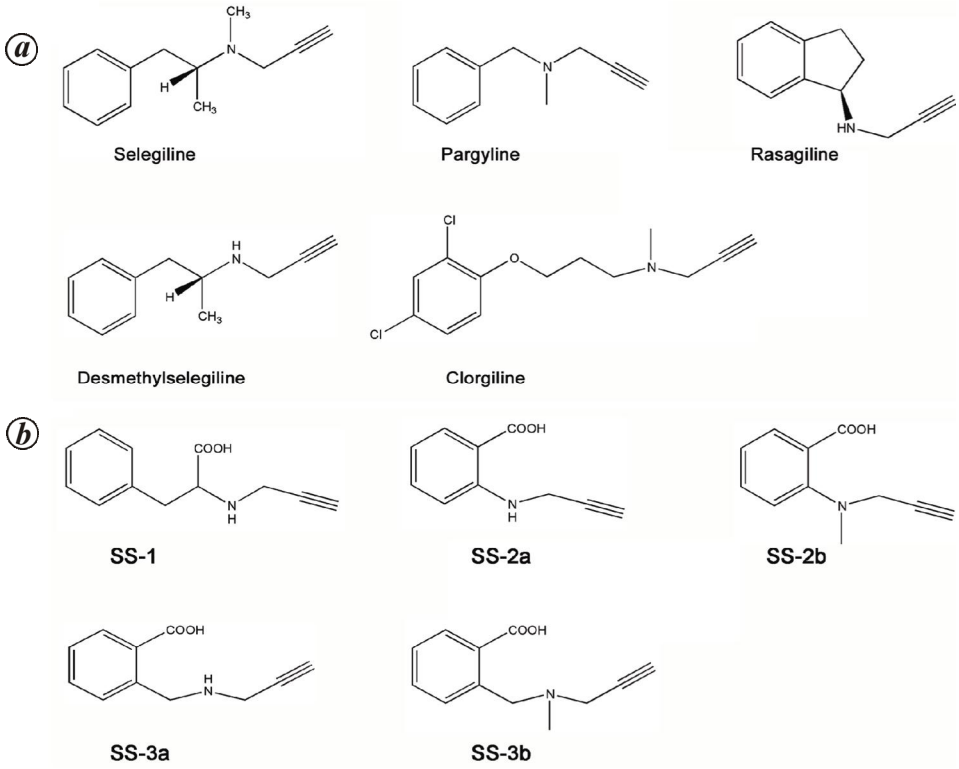

Figure 3. ***a***, Mechanism-based inhibitors of mono amine oxidase (MAO) that are used as drugs. ***b***, Probable acetylenic amino acid inhibitors of SV-LAAO.

Organic extracts were dried over anhydrous Na_2SO_4. Solvents were evaporated under reduced pressure using a rotary evaporator (EYELA N1000, USA). Progress of the reactions was monitored by TLC, performed on Kieselgel 60 F_{254} precoated silica gel plates and samples were detected by short UV light (254 nm). Column chromatography was performed using 100–200 μm mesh silica gel. ^1H and ^{13}C NMR spectra were run at 300 MHz. Chemical shifts (δ) were reported in ppm (parts per million) downfield from TMS; multiplicities are abbreviated as: s, singlet; d, doublet; t, triplet; q, quartet; m, multiplet; dd, doublet of doublet, and brs, broad. Mass spectra were generated from Waters Qtof Micromass (USA) with capillary and sample cone voltage of 3000 and 45 V respectively.

Synthesis of SS-1 (N-propargyl phenylalanine): The steps are outlined in Scheme 1 (ref. 31). Phenyl pyruvic acid (656 mg, 4 mmol) and $NaBH_3CN$ (390 mg, 6 mmol) were taken in 20 ml dry methanol. Propargylamine (320 μl, 5 mmol) in 5 ml of dry methanol was slowly added and the mixture was stirred for 48 h. Thereafter, conc. HCl (5 ml) was added and stirred for 1 h. The solution was evaporated. The residue was dissolved in 3 ml of water and applied to Dowex-50 (H^+-form, 100 milliequivalent capacity) column. After loading, the column was washed with 500 ml distilled water and the amino acid derivative was eluted with 300 ml of 1 N NH_4OH (ref. 31). The fraction was evaporated to yield an amorphous solid (439 mg, 48%).

Synthesis of SS-2a and SS-2b: The steps are outlined in Scheme 2 (ref. 32). Briefly, methyl anthranilate (5 g, 33.07 mmol) and anhydrous K_2CO_3 (4.56 g, 33.07 mmol) in dry DMF (20 ml) were stirred for 8 h. Propargyl bromide (4.72 g, 39.68 mmol) in dry DMF (10 ml) was added slowly under ice-cold condition over 20 min. The mixture was heated at 80°C for 48 h with constant stirring. DMF was evaporated and the compound was purified by silica gel chromatography using pet ether : chloroform (1 : 1) as solvent to yield yellowish-white crystalline 2-prop-2-ynylamino-benoic acid methyl ester (43.06 g; 68.9%).

Methyl 2-(*N*-methyl-*N*-prop-2′-yne) aminobenzoate was obtained by the reaction of methyl 2-(*N*-prop-2′-yne) aminobenzoate with methyl iodide[32]. Briefly, 2-prop-2-ynylaminobenoic acid methyl ester (0.6 g, 3.17 mmol) and anhydrous K_2CO_3 (0.438 g, 3.17 mmol) in dry DMF (2.5 ml) were stirred for 8 h. Methyl iodide (1.42 g, 10 mmol) was added slowly under ice-cold condition over 20 min. The reaction mixture was heated at 60°C for 24 h. The residue, after removal of DMF, was extracted with chloroform (3 × 10 ml). The combined chloroform layers were washed with water (2 × 20 ml) and dried over anhydrous Na_2SO_4. After removal of solvent, the residue was purified by silica gel (100–200 mesh) column

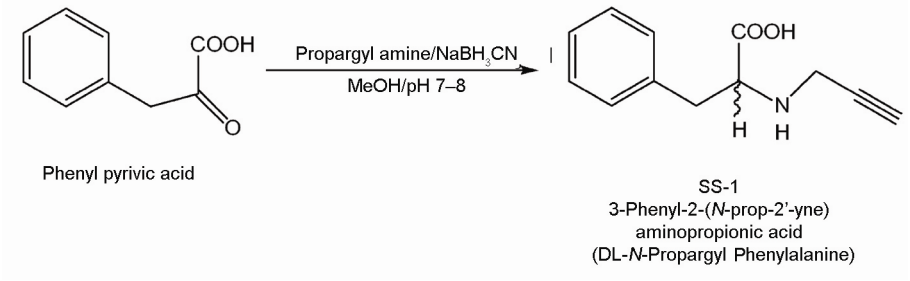

Scheme 1. Synthesis of SS-1.

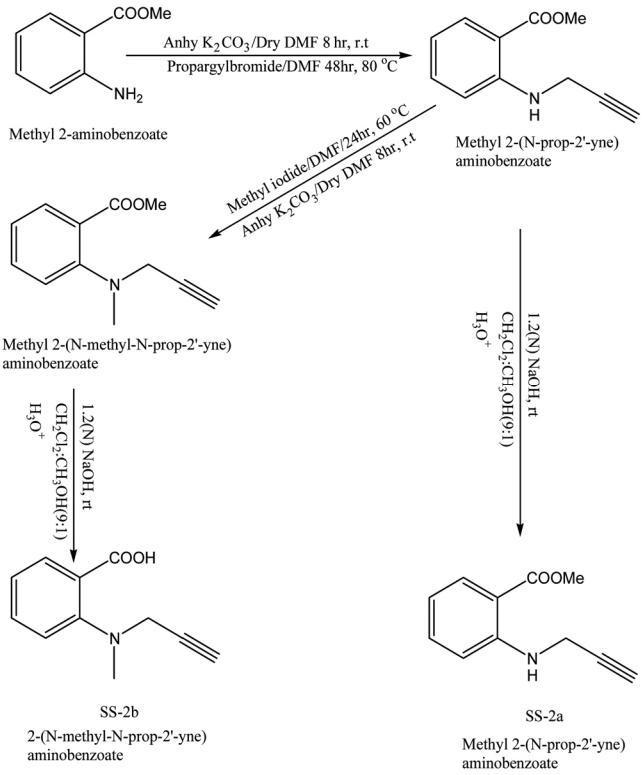

Scheme 2. Synthesis of SS-2a and SS-2b.

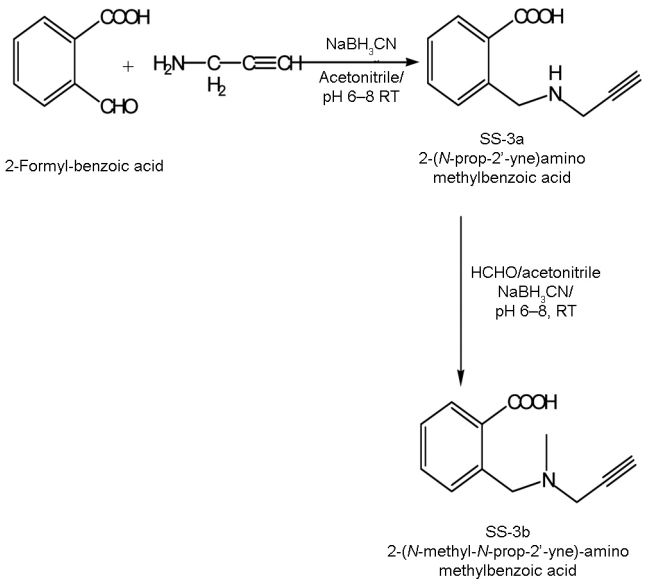

Scheme 3. Synthesis of SS-3a and SS-3b.

chromatography using 3 : 1 chloroform : pet ether (60–80°C). Solvent was removed to get methyl 2-(*N*-prop-2′-yne) aminobenzoate as a oily liquid (0.39 g; 65%).

Methyl 2-(*N*-prop-2′-yne) aminobenzoate (1.0 g, 5.3 mmol) and methyl 2-(*N*-methyl-*N*-prop-2′-yne) aminobenzoate (0.39 g, 1.92 mmol) were separately dissolved in 10 ml (9 : 1 CH_2Cl_2 : MeOH) solution and 1.0 g of NaOH was added under stirring condition to maintain NaOH concentration at 1.2 N. Na-salt of the acid slowly precipitated[33]. The reaction mixture was filtered-off and the residue was washed with 10 ml (9 : 1 CH_2Cl_2 : MeOH) to get 2-(*N*-prop-2′-yne) aminobenzoic acid (SS-2a) and 2-(*N*-methyl-*N*-prop-2′-yne) aminobenzoic acid (SS-2b). The yield was around 90% for both ester hydrolysis.

Synthesis of SS-3a and SS-3b: The steps are outlined in Scheme 3. 2-Formylbenzoic acid (750 mg, 5 mmol) and $NaBH_3CN$ (520 mg, 8 mmol) were taken in 20 ml of dry acetonitrile. Propargylamine (320 µl, 5 mmol) in 5 ml dry methanol was slowly added to it and the mixture was stirred for 48 h. Thereafter, glacial acetic acid (0.5 ml) was added dropwise over 10 min and stirred for 22 h. After removal of the solvent, the residue was purified by passing through silica gel column (100–200 mesh) using ethyl acetate : *n*-hexane (1 : 1) as solvent. Removal of the solvent yielded 2-(*N*-prop-2′-yne) aminomethylbenzoic acid (SS-3a) as white sticky solid (209 mg, 20%).

2-(*N*-prop-2′-yne) aminomethylbenzoic (100 mg, 0.49 mmol) and $NaBH_3CN$ (130 mg, 2 mmol) were added to dry acetonitrile (5 ml) and formaldehyde (0.2 ml, 2.5 mmol) and stirred for 24 h. After removal of the solvent, the residue was purified by silica gel chromatography (mesh 100–200) using ethyl acetate: methanol (9 : 1) as solvent. Removal of the solvent yielded pure 2-(*N*-methyl-*N*-prop-2′-yne) aminomethylbenzoic acid (SS-3b) as a yellowish oily liquid (27 mg; 25%).

Spectral data of synthetic compounds: SS-1: Mass: *m*/*z* of $[M + H]^+$, expected, 204.12 Da; observed, 204.06 Da. NMR: ^{1}H NMR of SS-1. δ 7.0–7.5 (m, 4H, Ar), 2.46 (s, 1H, CCH), 2.81–2.83 (d, 2H, NCH_2), 3.16–3.34 (q, 1H, NH), 3.43–3.48 (t, 1H, $CHCH_2Ph$).

SS-2a: Mass: *m*/*z* of $[M + Na]^+$, expected, 212.10 Da; observed, 212.02 Da. NMR: ^{1}H NMR of SS-2a. δ 7.97–7.99 (d, 1H, Ar), 7.42–7.47 (t, 1H, Ar), 6.79–6.82 (d, 1H, Ar), 6.67-6.72 (t, 1H, Ar), 5.30 (s, 1H, NH), 4.033 (s, 2H, NCH_2), 2.22 (s, 1H, CCH).

SS-2b: Mass: *m*/*z* of $[M + H]^+$, expected, 190.11 Da; observed, 190.05 Da. NMR: ^{1}H NMR of SS-2b. δ 6.79–7.32 (m, 3H, Ar), 7.45–7.50 (t, 1H, Ar), 4.11 (s, 2H, NCH_2), 2.85 (s, 3H, NCH_3), 2.21 (s, 1H, CCH).

SS-3a: Mass: *m*/*z* of $[M + CAN + H]^+$, expected, 231.13 Da; observed, 231.04. NMR: ^{1}H NMR of SS-3a. δ 7.37–7.68 (m, 4H, Ar), 2.43–2.45 (d, 2H, NCH_2), 2.16–2.17 (d, 2H, NCH_2), 1.89 (s, 1H, CCH), 1.15–1.21 (h, 1H, NH).

SS-3b: Mass: *m*/*z* of to $[M+ A CN + H]^+$, expected, 245.14 Da; observed, 245.04. NMR: ^{1}H NMR of SS-5b. δ 7.45–8.00 (m, 4H, Ar), 3.87 (s, 2H, CH_2Ph), 3.32 (s, 2H, NCH_2), 2.816 (s, 3H, NCH_3), 2.001 (s, 1H, CCH).

Assay of LAAO

LAAO was assayed using arsenate–borate method[34]. Catalysis of L-Phe by LAAO generates phenylpyruvic acid which forms a complex with boric acid that absorbs at 300 nm. The assay mixture contains 0.96 M Na-arsenate, 0.8 M boric acid, 1 mM of L-Phe and 1.2 units of catalase in 50 mM phosphate, pH 7.5. Catalase removed H_2O_2 to prevent interference with phenylpyruvic acid. The reaction was initiated with 0.05 U of LAAO and followed at 25°C using an Analytik Jena Specord 200 spectrophotometer (Germany) attached with a circulating water bath (Polyscience, USA).

Results

Protein sequence alignment and homology modelling

Multiple sequence alignment of *Crotalus adamanteus* LAAO with other snake-venom LAAOs using ClustalW2.1 showed >84% sequence similarity (Table 1). Homology model of *Crotalus adamanteus* LAAO was built using *Calloselasma rhodostoma* (PDB ID: 2IID) as the template structure. Predicted structure quality was good as judged through ProSA tool. ProSA tool graph showed overall quality of model structure and the location of the *z*-score. A plot of single residue energies usually contains large fluctuations and is of limited value for model evaluation. Hence, the plot is smoothed by calculating the average energy over each 40-residue where negative energy value throughout the protein sequence justifies the quality of the model (Figure 4 *a*). The *z*-score value –11.18 was in the range of native conformation of all proteins in the PDB, for which the *z*-score is represented by blue dots, deep blue for NMR and light blue for X-ray structures (Figure 4 *b*). In addition, the overall fold of the model is similar to that of LAAO from *Calloselasma rhodostoma* venom (Figure 4 *c*). The RMS deviations for all atoms obtained by the superposition of the three main domains, viz. FAD binding, substrate-binding and helical domains of *Crotalus adamanteus* LAAO models and those from *Calloselasma rhodostoma* LAAO crystal structure confirm high degree of structural similarity between these enzymes (Table 2).

Docking

Binding modes of the proposed inhibitors were predicted by molecular docking of the inhibitors with *Crotalus adamanteus* LAAO model using Autodock Vina[28]. Compounds SS-1 to SS-3b were successfully docked onto the active site of LAAO. Table 3 shows the results of the docking experiments in terms of calculated free energy of

Table 1. SV-LAAO sequence alignment

Identification no.	Species	Amino acid length	Crystal structure
1	*Crotalus adamanteus*	516	–
2	*Agkistrodon halys*	486	1REO
3	*Vipera ammodytes*	485	3KVE
4	*Calloselasma rhodostoma*	516	2IID

Sequence alignment	Alignment score
1 : 2	85.8
1 : 3	83.7
1 : 4	84.4

Table 2. RMS deviations of the three main regions – FAD-binding domain, substrate-binding domain and helical domain of LAAO as calculated from superposition of *Crotalus adamanteus* LAAO model with *Calloselasma rhodostoma* LAAO structure (PDB : 2IID)

	Residue	RMSD value (Å)
FAD-binding domain	35–64	0.447
	242–318	0.555
	446–471	0.582
Substrate-binding domain	5–25	0.555
	73–129	0.589
	233–236	0.221
	323–420	0.628
Helical domain	130–230	0.613

binding. OAB was docked into the active site of LAAO (Figure 5 *a*). This inhibitor lies within the active site nearest to the isoalloxazine ring with C1 positioned at 4.4 Å away from N5 of FAD. This is comparable to the distance of 3.9 Å observed in the crystal structure[9]. Furthermore, H-bond interactions between carbonyl group and Tyr327 (3.9 Å) and Arg90 (3.1 Å) may stabilize the complex along with the π–π stacking interaction of the phenyl ring of Phe227. Figure 5 *b* shows final docked position of SS-1, where the propargyl group is extended away from FAD making π–π stacking interaction with Tyr327. Other principal interactions of compounds SS-1 were the same as those of L-Phe in the crystal structure where the carboxylate group is engaged in hydrogen-bond interactions with the guanidinium group of Arg90 and the hydroxyl group of Tyr327. Also, the amine group of L-Phe may be stabilized by H-bond with the carbonyl oxygen atom of Gly464. In case of SS-2a and SS-2b, the propargyl group was oriented a little away from the FAD cofactor, while the other major interactions were the same as that of OAB (Figure 5 *c* and *d*). It was observed that the phenyl ring and propargyl group of SS-3a form π–π stacking interactions with Phe227 and Tyr327 respectively, and the carboxyl group is involved in H-bonding with Arg90 (2.8 Å; Figure 5 *e*). The phenyl ring of SS-3b is sandwiched between Phe227 and His223 (Figure 5 *f*). The propargyl group is extended away from FAD and forms π–π stacking with Tyr327, and the H-bond interaction of the carboxylate group is the same as that of SS-3a.

Enzyme kinetics

The synthetic compounds were evaluated for their LAAO inhibitory activity using arsenate–borate method. The usual assay protocol using HRP as coupling enzyme could not be applied as some of the synthetic compounds interfered. SS-1 (5 mM) acted as a very weak substrate. Its conversion by LAAO (0.1 U) could be detected only after incubation for 1 h at ambient temperature. This indicates that SS-1 competed with L-Phe at high concentration. So, further investigation was discontinued. The rate of change of absorbance corresponding to the formation of phenyl pyruvate–borate complex in presence of 0.5 mM SS-1, 0.5 mM SS-2a, 0.25 mM SS-2b and 0.1 mM of both SS-3a and SS-3b respectively is shown (Figure 6 *a*). It was observed that only SS-2a and SS-2b showed inhibition of LAAO. To identify the nature of inhibition, Lineweaver–Burk plots were generated with variable concentration of SS-2a, where a mixed type of inhibition was observed (Figure 6 *b*). Similar pattern was generated for SS-2b. IC_{50} values of SS-2a and SS-2b were comparable to that of OAB, being 0.288 and 0.269 µM respectively versus 0.229 µM for OAB (Figure 6 *c* and Table 3).

Table 3. AutoDock Vina estimated free energies of binding (ΔG_b) of different ligands with the active site of *Crotalus adamanteus* LAAO model

Ligand	ΔG_b (kcal/mol)	IC_{50} (µM)
L-Phenylalanine	–7.0	–
OAB	–6.0	7.9
SS-1	–7.8	–
SS-2a	–6.8	1.6
SS-2b	–6.4	3.3
SS-3a	–7.6	–
SS-3b	–7.7	–

Discussion

The objective of this study was to design and synthesis suicide inhibitors of SV-LAAO from the knowledge of the catalytic mechanism coupled with bioinformatics tools. The structure of LAAO from *Calloselasma rhodostoma* co-crystallized with the substrate L-Phe has been recently solved at a resolution of 1.8 Å (ref. 10). Two flexible residues, His223 and Arg322, were identified along the funnel-like entry pathway of the substrate into the active site. Significant movement was observed for His223; its side-chain rotates ~90° within the binding cavity. The substrate, L-Phe remains bound to the reface of the cofactor FAD and the side chain of L-Phe is extended away from the cofactor making slight angle with the imidazole ring of His223 (Figure 2). Although complete π-stacking interaction does not occur, these contacts aid in orienting the substrate at the catalytic centre. The carboxylate group is involved in a salt-bridge interaction with the guanidinium group of Arg90 and a H-bond with the OH-group of Tyr327. The α-C atom of the substrate, representing the site of oxidative attack, is positioned over the isoalloxazine ring at a distance of 3.1 Å from N5 of FAD. The amino group of the substrate forms hydrogen-bond interaction with the carbonyl oxygen atom of Gly464. Finally, the phenyl ring of the substrate participates in hydrophobic interaction with the side-chain of Ile374 and Phe227 and with the changed conformation of Arg322 and His223 (ref. 10). OAB, a known reversible inhibitor of LAAO, also binds at the catalytic site with similar binding interactions[9]. Residues Arg90, His223, Tyr327 and Gly464 are responsible for the contact of three OAB molecules in the funnel-shaped channel. These residues interact with L-Phe and guide the substrate to the active site. All the structural information conveys the message that L-Phe and OAB would be the best scaffolds over which suicide inhibitor structure could be built. Accordingly the crystal structure of LAAO from *Calloselasma rhodostoma*, His-223 and Arg-322 were identified as two flexible residues. In the homology model developed, similar conditions were retained. The interactions with OAB, a known reversible inhibitor of LAAO, were also studied and they were in agreement

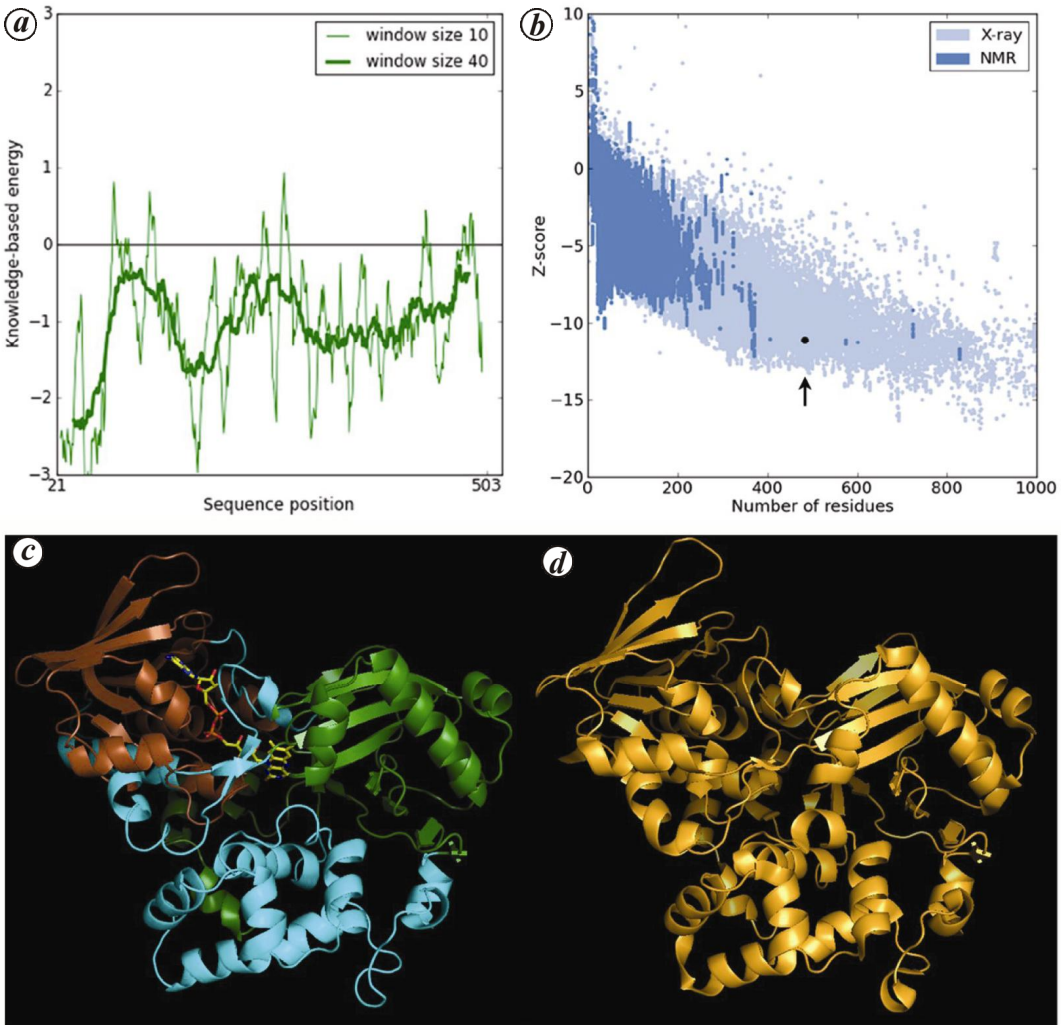

Figure 4. Validation of the homology model of *Crotalus adamanteus* LAAO by ProSA tool. ***a***, Knowledge-based average energy amino acid residues with sequence position. Thin line indicates average energy for 10 residues, while thick line indicates average energy for 40 residues. ***b***, *z*-score of proteins plotted against the number of residues. Light and deep blue spots represent the *z*-score value of X-ray and NMR-determined protein structures enlisted in the PDB. The black dot marked by the arrow indicates the *z*-score of *Crotalus adamanteus* LAAO homology model. ***c***, Homology model of *Crotalus adamanteus* LAAO showing three main domains: FAD-binding domain (brown); substrate-binding domain (green) and helical domain (blue). FAD is shown in yellow stick. ***d***, Crystal structure of *Calloselasma rhodostoma* LAAO (FAD not shown).

with the crystal structure. So, the incorporation of flexibility in these residues did not affect binding of the synthesized compounds to the enzyme.

Increasing success of acetylenic suicide inhibitors of MAO over the past few decades has generated great interest towards designing of acetylenic moiety-based suicide inhibitor of LAAO. Compounds SS-1, SS-2a and SS-2b were designed by mimicking the structure of L-Phe and OAB. Apart from these, two other structures – SS-3a and SS-3b – were designed based on aromatic phenyl ring along with carboxyl and amine functional groups, as discussed previously. Our attempt to design and synthesize suicide substrate of LAAO by utilizing the crystallographic structure of the enzyme was not successful. However, this rational approach of designing inhibitors led to two potent reversible inhibitors, SS-2a and SS-2b, with IC_{50} values of 1.6 and 3.3 μM respectively.

Multiple sequence alignment demonstrates high homology of LAAO from *Crotalus adamanteus* venom with that from *Agkistrodon halys* and *Calloselasma rhodostoma* venom. The homology model built through CPH on-line server has *z*-score very close to that of the native protein crystal structure. The *z*-score indicates overall quality of the model[26,27]. It can be used to check whether the *z*-score of the input structure is within the range of scores typically found for all native proteins of similar size reported in the PDB. The plot of residue scores shows local model quality by plotting energies as a function of amino acid sequence position *i*. In general, positive values correspond to problematic or erroneous

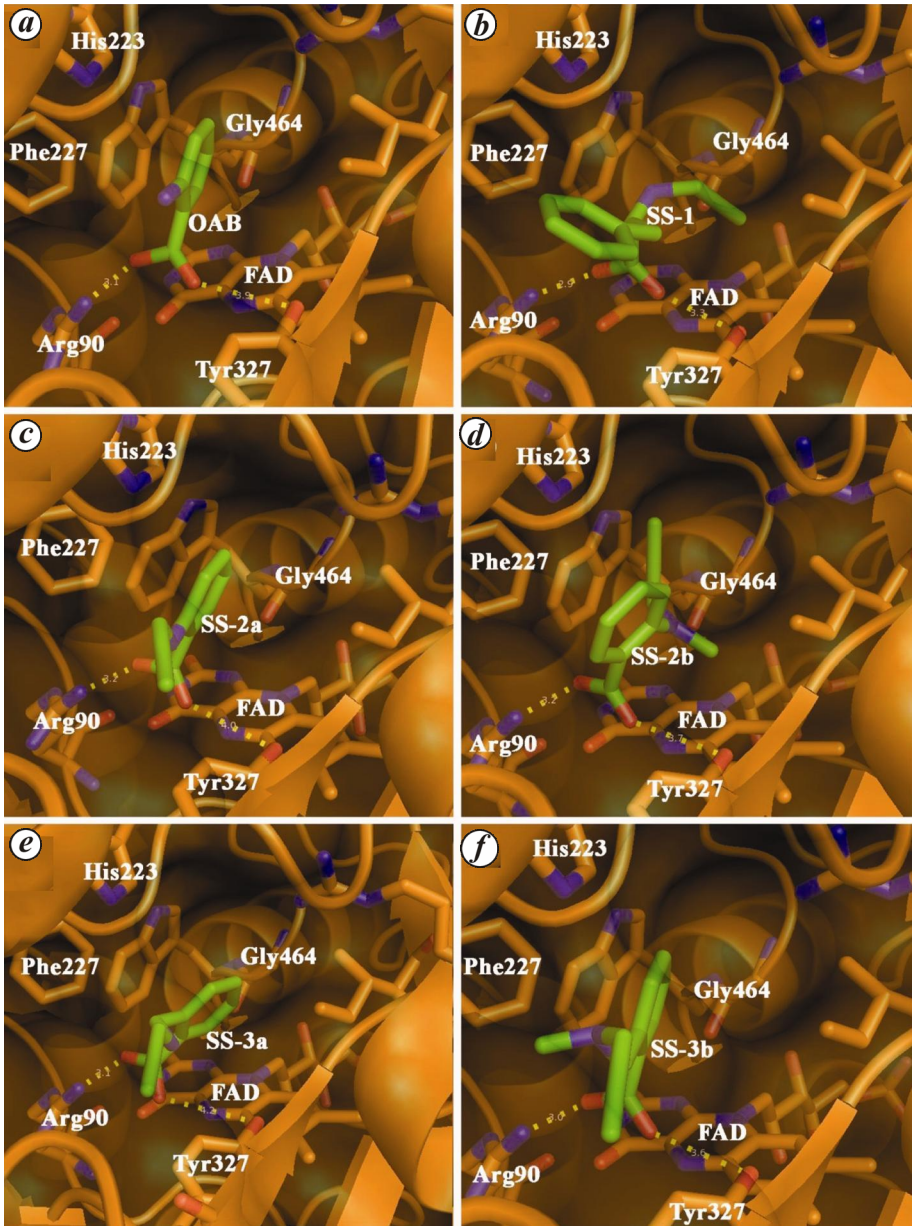

Figure 5. Docking of (***a***) OAB, (***b***) SS-1, (***c***) SS-2a, (***d***) SS-2b, (***e***) SS-3a and (***f***) SS-3b with *Crotalus adamanteus* LAAO homology model. The important residues of the enzyme and the ligands are depicted by stick model. Ligands and the flexible residues are presented in white. Oxygen and nitrogen atoms are presented in red and blue respectively.

parts of the input structure. A plot of single residue energies usually contains large fluctuations and is of limited value for model evaluation. Hence average energy over each 40-residue fragment (i, $i + 39$) is calculated, which is then assigned to the 'central' residue of the fragment at position $i + 19$ (Figure 4 *a*, thick line). A second line with a smaller window size of 10 residues is shown in the background of the plot (Figure 4 *a*, thin line). The calculated RMS deviation of the protein residue along three main domains, obtained through superposition of the homology model with the crystal structure, confirms high degree of structure similarity (Table 2).

To have insight into different binding modes of proposed inhibitors at the catalytic site of LAAO, AutoDock Vina simulation program was used. Flexibility of ligand was considered during docking experiments. Addition of propargyl group to the α-amino group of L-Phe scaffold was not promising in converting it to an inhibitor. Moreover, its substrate-like character was significantly reduced. The phenomenon can be visualized by assuming that the increase in size of the ligand by incorporation of the propargyl group makes it large so that it neither enters into the active site funnel nor orients properly in the active site for hydride transfer. This is in accordance with

the docking study where it was observed that SS-1 is not well accommodated in the active site. The phenyl ring emerged out of the catalytic pocket making the α-C atom extended away from N5 atom of isoalloxazine ring, whereas in case of SS-2a and SS-2b, the hydrophobicity imparted by the propargyl group does not make much difference with respect to OAB in terms of inhibition. However, no irreversible inactivation was observed for SS-2a and SS-2b. Thus, more than one SS-2a may bind to the catalytic funnel of the enzyme as observed from the crystal structure of LAAO with OAB[9]. Compound SS-3a neither inhibited the enzyme nor acted as a substrate. This fact is supported by the docking study where the molecule undergoes π–π stacking interaction with Phe227 and orients itself away from the catalytic pocket.

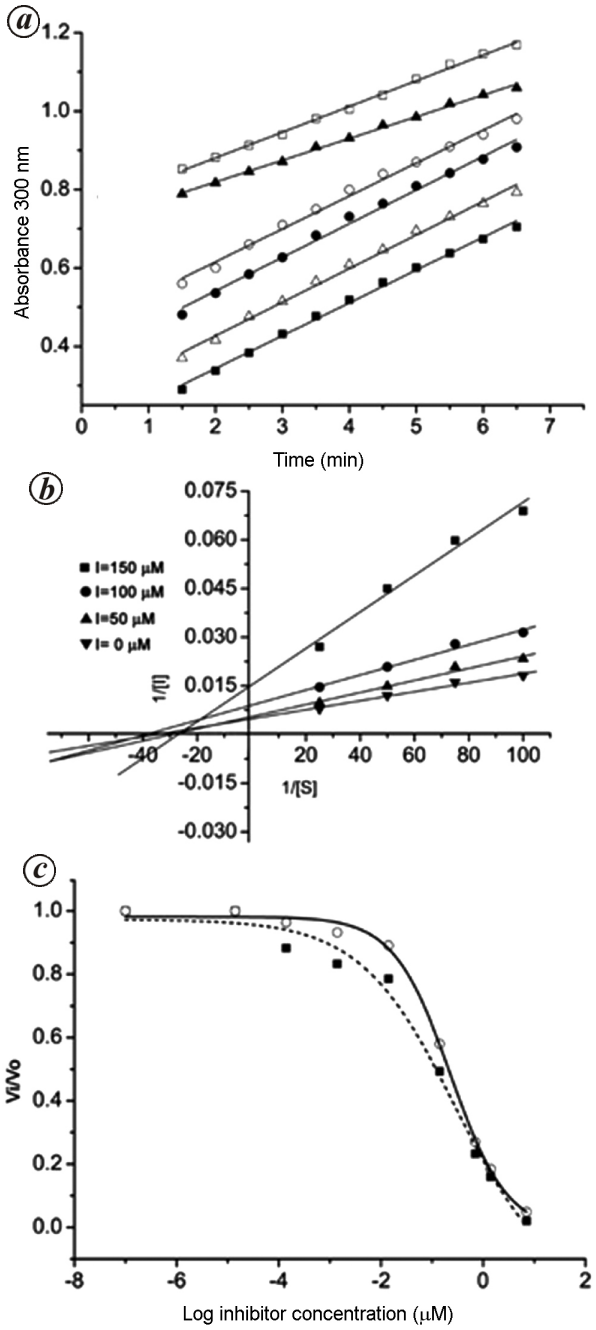

Figure 6. ***a***, Time kinetics of catalysis of LAAO with 1 mM L-Phe as substrate (solid cube), in the presence of 0.5 mM of SS-1 (solid circle) 0.5 mM SS-2a (solid triangle), 0.25 mM SS-2b (open cube), 0.1 mM SS-3a (open triangle) and SS-3b (open circle). Except SS-2a and SS-2b, no ligand acted as an inhibitor. ***b***, Lineweaver–Burk plot of LAAO with variable concentration of SS-2a that shows a mixed type of inhibition. ***c***, Dose–response curve of OAB and SS-2a shows similar potency for inhibiting LAAO. IC_{50} values are 0.229 and 0.288 µM respectively. To avoid confusion the curve for SS-2b is not shown, which has an IC_{50} value of 0.269 µM.

We observed similar set of interactions for most of these compounds in the docking models where SS2 acts as an inhibitor and but not SS3. This may be attributed to the fact that SS2 is a derivative of L-Phe, which is a good substrate of LAAO, while SS3 is a derivative of OAB. Absence of α-C atom in OAB hinders its binding at the catalytic site in a substrate-like fashion. These point towards the fact that its derivatives might not act as favourably as inhibitors. This is a limitation of docking studies of inhibitors which sometimes inadvertently show results that are not corroborated in enzyme assay. Further, in the background that 2–3 OAB molecules are accommodated in the catalytic funnel of LAAOs, there remains a possibility that there are multiple binding sites of the inhibitors in the catalytic funnel. We have not analysed incorporation of inhibitor/s at sites other than the conversion site, as these associations will not lead to irreversible inactivation of the enzyme (as suicidal substrate). For the same reason, we have not analysed simultaneous application of two inhibitors in the model.

In summary, molecular modelling gives useful information about the receptor pocket like hydrophobic/hydrophilic patches and the type of ligands that can be accommodated in that pocket along with different types of receptor–ligand binding interactions. So designing of inhibitors of LAAO from the knowledge of crystal structure and the binding interaction of the substrate (L-Phe) in the catalytic site has a fair chance of success. It was assumed that the probable inhibitors would be recognized by the catalytic pocket of LAAO, since they were based on the structural and functional features of the substrate. This was evident from the efficient binding interactions observed in the docking study for most of the proposed inhibitors, but only two of them inhibit the enzyme. This is because a protein and its catalytic pocket, in contrast to a crystal structure, are not static but dynamic in nature. So, docking studies with mere incorporation of flexibility of the catalytic residues or ligands may/may not lead to the development of new inhibitors. It should be complemented by enzyme assay. In this case, the designed molecules emerged as reversible inhibitors indicating that additional refinement of the structures is required to convert them to suicidal substrates. Prototype static crystallographic structures of proteins may not be adequate to accommodate their dynamic nature.

1. Vaiyapuri, S., Wagstaff, S. C., Watson, K. A., Harrison, R. A., Gibbins, J. M. and Hutchinson, E. G., Purification and characterisation of rhiminopeptidase A, a novel aminopeptidase from the venom of *Bitis gabonica*. *PLoS Neg. Dis.*, 2010, **4**, e796.
2. Curti, B., Ronchi, S. and Simonetta, M. P., D- and L-amino acid oxidases. In *Chemistry and Biochemistry of Flavoenzymes* (ed. Muller, F.), CRC Press, Boca Raton, FL, 1992, vol. 3, pp. 69–94.
3. Du, X. Y. and Clemetson, K. J., Snake venom L-amino acid oxidases. *Toxicon*, 2002, **40**, 659–665.
4. Suhr, S. M. and Kim, D. S., Identification of snake venom substrate that induces apoptosis. *Biochem. Biophys. Res. Commun.*, 1996, **224**, 134–139.
5. Suhr, S. M. and Kim, D. S., Comparison of the apoptotic pathways induced by L-amino acid oxidase and hydrogen peroxidase. *J. Biochem.*, 1999, **125**, 305–309.
6. Torii, S. *et al.*, Molecular cloning and functional analysis of apoxin I, a snake venom-derived apoptosis-inducing factor with L-amino acid oxidase activity. *Biochemistry*, 2000, **39**, 3197–3205.
7. Ande, S. R., Kommoju, P. R., Draxl, S., Murkovic, M., Macheroux, P., Ghisla, S. and Ferrando-May, E., Mechanisms of cell death induction by L-amino acid oxidase, a major component of ophidian venom. *Apoptosis*, 2006, **11**, 1439–1451.
8. Mandal, S. and Bhattacharyya, D., Two L-amino acid oxidase isoenzymes from Russell's viper (*Daboia russelli russelli*) venom with different mechanism of inhibition by substrate analogs. *FEBS J.*, 2008, **275**, 2078–2095.
9. Pawelek, P. D., Cheah, J., Coulombe, R., Macheroux, P., Ghisla, S. and Vrielink, A., The structure of L-amino acid oxidase reveals the substrate trajectory into an enantiomerically conserved active site. *EMBO J.*, 2000, **19**, 4204–4215.
10. Moustafa, I. M., Foster, S., Lyubimov, A. Y. and Vrielink, A., Crystal structure of LAAO from *Calloselasma rhodostoma* with an L-phenylalanine substrate: insight into structure and mechanism. *J. Mol. Biol.*, 2006, **15**, 991–1002.
11. Franca, S. C., *et al.*, Molecular approaches for structural characterization of Bothrops L-amino acid oxidases with anti protozoal activity: cDNA cloning, comparative sequence analysis, and molecular modelling. *Biochem. Biophys. Res. Commun.*, 2007, **355**, 302–306.
12. Maycock, A. L. and AIDer, J., Structure of (flavoprotein-) inactivator model compound. *J. Am. Chem. Soc.*, 1975, **97**, 2270–2272.
13. Walsh, C. T., Schonbrunn, A., Lockridge, O., Massey, V. and Abeles, R. R., Inactivation of a flavoprotein, lactate oxidase, by an acetylenic substrate. *J. Biol. Chem.*, 1972, **247**, 6004–6006.
14. Schonbrunn, A., Abeles, R. H., Walsh, C. T., Ghisla, S., Ogata, S. H. and Massey, V., The structure of the covalent flavin adduct formed between lactate oxidase and suicide substrate 2-hydroxy-3-butynoate. *Biochemistry*, 1976, **15**, 1798–1807.
15. Chen, Z. W., Zhao, G., Martinovic, S., Jorns, M. S. and Mathews, F. S., Structure of the sodium borohydride-reduced *N*-(cyclopropyl) glycine adduct of the flavoenzyme monomeric sarcosine oxidase. *Biochemistry*, 2005, **44**, 15444–15450.
16. Silverman, R. B., Mechanism-based enzyme inactivator. *Methods Enzymol.*, 1995, **249**, 240–280.
17. Walsh, C. H., Recent developments in suicide substrate and other active site-directed inactivating agents of specific target enzymes. *Horiz. Biochem. Biophys.*, 1977, **3**, 36–81.
18. Binda, C., Hubalek, F., Li, M., Herzir, Y., Sterling, J., Edmondson, D. E. and Mattevi, A., Crystal structure of monoamine oxidase B in complex with four inhibitors of the *N*-propargylaminoindan class. *J. Med. Chem.*, 2004, **47**, 1767–1774.
19. Binda, C., Hubalek, F., Li, M., Herzir, Y., Sterling, J., Edmondson, D. E. and Mattevi, A., Binding of rasagiline-related inhibitors to human monoamine oxidase: a kinetic and crystallographic analysis. *J. Med. Chem.*, 2005, **48**, 8148–8154.
20. Youdim, M. B. H., Edmondson, D. and Tipton, K. F., The therapeutic potential of monoamine oxidase inhibitors. *Nat. Rev. Neurosci.*, 2006, **7**, 295–309.
21. Mitra, J. and Bhattacharyya, D., Irreversible inactivation of snake venom L-amino acid oxidase by covalent modification during catalysis of L-propargylglycine. *FEBS Open Biol.*, 2013, **3**, 135–143.
22. Zhang, H. *et al.*, Purification, partial characterization, crystallization and structural determination of AHP-LAAO, a novel L-amino acid oxidase with cell apoptosis-inducing activity from *Agkistrodon halys pallas* venom. *Acta Crystallogr.*, 2004, **60**, 974–977.
23. Georgieva, D., Murakami, M., Perband, M., Arni, R. and Betzel, C., The structure of native L-amino acid oxidase, the major component of the Vipera ammodytes ammodytes venomic, reveals dynamic active site and quaternary structure stabilization by divalent ions. *Mol. Biosyst.*, 2011, **7**, 379–384.
24. Arnold, K., Bordoli, L., Kopp, J. and Schwede, T., The SWISS-MODEL Workspace: a web-based environment protein structure homology modelling. *Bioinformatics*, 2006, **22**, 195–201.
25. Nielsen, M., Lundegaard, C., Lund, O. and Petersen, T. N., CPHmodels-3.0 – Remote homology modelling using structure guided sequence profiles. *Nucleic Acids Res.*, 2010, **38**, W576–W581.
26. Wiederstein, M. and Sippl, M. J., ProSA-web: interactive web service for the recognition of errors in the three-dimensional structures of proteins. *Nucleic Acids Res.*, 2007, **35**, W407–W410.
27. Sippl, M. J., Recognition of errors in three-dimensional structure of proteins. *Proteins*, 1993, **17**, 355–362.
28. Trott, O. and Olson, A. J., AutoDock Vina: improving the speed and accuracy of docking with a new scoring function, efficient optimization and multithreading. *J. Comput. Chem.*, 2010, **31**, 455–461.
29. Morris, G. M., Huey, R., Lindstrom, W., Sanner Belew R. K., Goodsell, D. S. and Olson, A. J., Autodock 4 and Autodocktools 4: automated docking with selective receptor flexibility. *J. Comput. Chem.*, 2009, **16**, 2785–2791.
30. The PyMOL Molecular Graphics System, version 1.5.0.4, Schrödinger, LLC.
31. Hirs, C. H. W., Moore, S. and Stein, W. H., Isolation of amino acid by chromatography on ion exchange columns; use of volatile buffers. *J. Biol. Chem.*, 1952, **195**, 669–683.
32. Kundu, N. G. and Chaudhuri, G., Copper-catalysed heteroannulation with alkynes: a general and highly region and stereoselective method for the synthesis of (E)-2-(2-arylvinyl) quinazolinones. *Tetrahedron*, 2001, **57**, 6833–6842.
33. Theodorou, V., Skobridis, K., Tzakos, A. G. and Ragoussis, V., A simple method for the alkaline hydrolysis of esters. *Tetrahedron*, 2007, **48**, 8230–8233.
34. Wellner, D. and Lichtenberg, L. A., Assay of amino acid oxidase. *Methods Enzymol. B*, 1971, **17**, 593–596.

ACKNOWLEDGEMENTS. J.M. and K.S. were supported by CSIR/UGC-NET fellowships. We thank our colleagues Mr Simanta Sarani Paul, Mr Biprashekhar Chakraborty and Mr Manidip Shasmal for help with modelling studies.

Received 26 March 2014; revised accepted 26 December 2014